



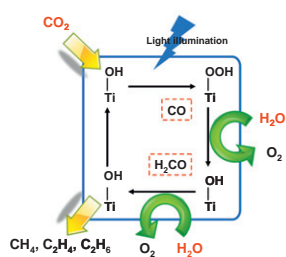
Journal of Catalysis Vol. 284, Issue 1, 2011

Contents

Mechanistic study of hydrocarbon formation in photocatalytic CO₂ reduction over Ti-SBA-15

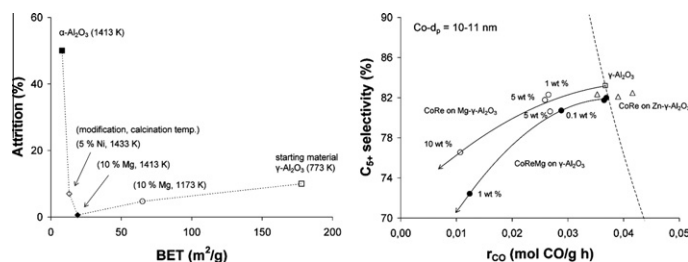
pp 1–8

Chieh-Chao Yang, Jarian Vernimmen, Vera Meynen, Pegie Cool, Guido Mul*

Carbon monoxide and formaldehyde are key intermediates in photocatalytic CO₂ reduction over Ti-SBA-15.**Modified alumina as catalyst support for cobalt in the Fischer–Tropsch synthesis**

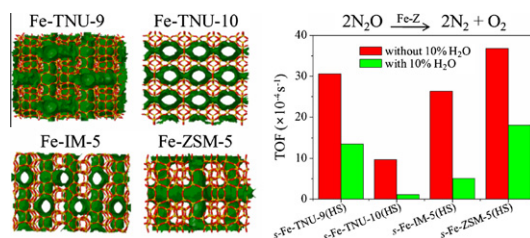
pp 9–22

Bjørn Christian Enger, Åse-Lill Fossan, Øyvind Borg, Erling Rytter, Anders Holmen*

Catalyst attrition as a function of the BET surface area and the C₅₊ selectivity as a function of the reaction rate for Mg, Zn, and Ni modifications.**Iron-substituted TNU-9, TNU-10, and IM-5 zeolites and their steam-activated analogs as catalysts for direct N₂O decomposition**

pp 23–33

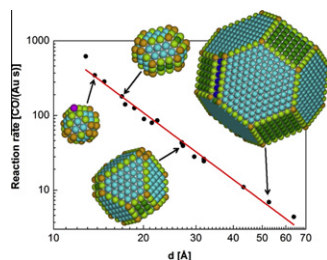
Jun Kyu Lee, Young Jin Kim, Heung-Ju Lee, Su Hyun Kim, Sung June Cho, In-Sik Nam, Suk Bong Hong*

Fe-TNU-9, Fe-TNU-10, and Fe-IM-5 zeolites containing both Fe and Al in framework positions have been hydrothermally synthesized, steam-activated, and tested as catalysts for direct N₂O decomposition. The physical state of iron species in these zeolites before and after steaming has been extensively characterized using various analytical tools.

Understanding the catalytic activity of gold nanoparticles through multi-scale simulations

pp 34–41

Simon H. Brodersen, Ulrik Grønbjerg, Britt Hvolbæk, Jakob Schiøtz*

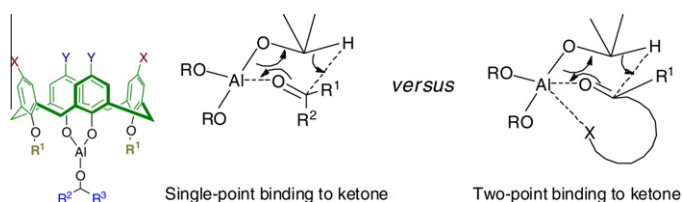


By calculating the atomic-scale shape of gold nanoparticles, and thus the number of catalytically active sites, it is possible to calculate their reactivity. The size dependence of the reactivity is in excellent agreement with experiments, allowing the conclusion that the reactivity is dominated by low-coordinated corner-like atoms.

MPV reduction using Al^{III}-calix[4]arene Lewis acid catalysts: Molecular-level insight into effect of ketone binding

pp 42–49

Partha Nandi, Yuriy I. Matvieiev, Vyacheslav I. Boyko, Kathleen A. Durkin, Vitaly I. Kalchenko, Alexander Katz*

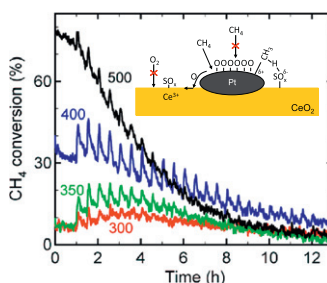


Al^(III)-calix[4]arene complexes act as site-isolated Lewis acid catalysts for homogeneous MPV reduction. Two-point versus one-point binding of ketone reactant is a crucial feature that controls the catalytic rate and enantioselectivity.

Sulfur promoted low-temperature oxidation of methane over ceria supported platinum catalysts

pp 50–59

Lisa Kylhammar, Per-Anders Carlsson*, Magnus Skoglundh

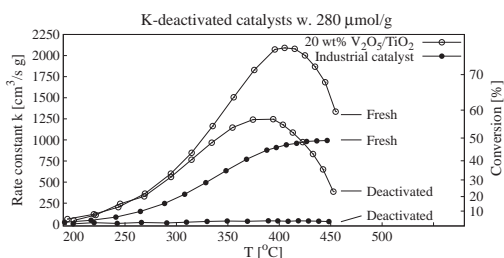


Methane oxidation over Pt/CeO₂ which is initially promoted by SO₂ pulsing, leading to formation of sulfates that facilitate oxygen spill-over and/or special sites at the platinum-ceria boundary for enhanced methane dissociation, and as a function of time on stream becomes gradually inhibited by sulfur exposure.

High performance vanadia-anatase nanoparticle catalysts for the Selective Catalytic Reduction of NO by ammonia

pp 60–67

Steffen B. Kristensen, Andreas J. Kunov-Kruse, Anders Riisager, Søren B. Rasmussen, Rasmus Fehrmann*

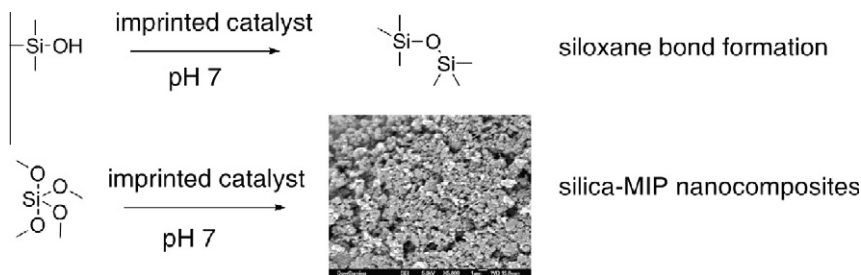


Nano-particle deNO_x catalysts showed high SCR activity and resistivity towards potassium poisoning compared to an industrial reference, upon impregnation by 280 μmole potassium/g of catalyst.

Biomimetic catalysis at silicon centre using molecularly imprinted polymers

pp 68–76

Vincenzo Abbate*, Alan R. Bassindale, Kurt F. Brandstadt, Peter G. Taylor*

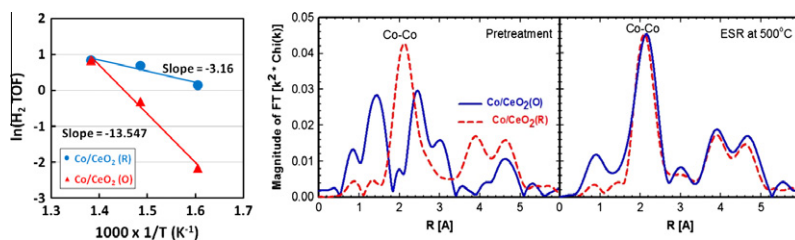


We report the first case of the use of Molecularly Imprinted Polymers for the biomimetic catalysis at silicon centre.

Ethanol steam reforming over Co-based catalysts: Investigation of cobalt coordination environment under reaction conditions

pp 77–89

Burcu Bayram, I. Ilgaz Soykal, Dieter von Deak, Jeffrey T. Miller, Umit S. Ozkan*

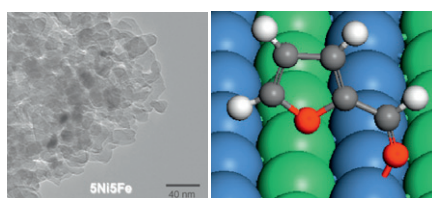


The transformations and state of cobalt species during steam reforming of ethanol were investigated over Co/CeO₂ catalysts pretreated with oxidation (O) and reduction (R) steps. Both catalysts were found to transform in situ to the same active phase under reaction conditions, exhibiting both CoO and Co⁰ species at steady state. The reforming performance of the two catalysts also converged to the same level, giving similar product yields.

Selective conversion of furfural to methylfuran over silica-supported Ni–Fe bimetallic catalysts

pp 90–101

Surapas Siththisa, Wei An, Daniel E. Resasco*

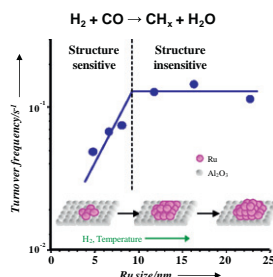


Left: TEM image of the NiFe bimetallic catalyst; Right: Optimized structure of furfural adsorbed on NiFe(1 1 1) surface.

Catalytic effects of ruthenium particle size on the Fischer–Tropsch Synthesis

pp 102–108

Juan María González Carballo, Jia Yang, Anders Holmen, Sergio García-Rodríguez, Sergio Rojas*, Manuel Ojeda, José Luis G. Fierro



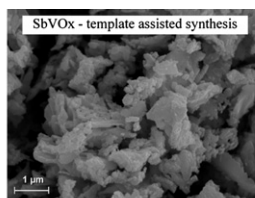
Ru size matters: This work investigates the catalytic consequences of Ru cluster size (4–23 nm) in the Fischer–Tropsch Synthesis. This reaction is structure sensitive when Ru < 10 nm: turnover frequency of CO consumption increases as Ru size increases from 4 to 10 nm, reaching a constant value for larger clusters.

Sb, V, Nb containing catalysts in low temperature oxidation of methanol – The effect of preparation method on activity and selectivity pp 109–123

Hanna Golinska-Mazwa, Piotr Decyk, Maria Ziolk*



- Low activity in methanol oxidation
- Selectivity to FA and DME



- High activity in methanol oxidation
 - Selectivity to FA and MF (with Nb - to DMM)
-